tvst

Article

Effects of Gelatin Methacrylate Hydrogel on Corneal Repair and Regeneration in Rats

Yun Chen[1,2,#], Lina Dong[1,#], Bin Kong[1], Yu Huang[3], Suyi Zhong[4], Che Connon[8], Jiaqi Tan[2], Siming Yang[5,*], Wei Sun[1,6,7,*], and Shengli Mi[1,2,6,*]

[1] Macromolecular Platforms for Translational Medicine and Bio-Manufacturing Laboratory, Tsinghua-Berkeley Shenzhen Institute, Shenzhen, P.R. China
[2] Open FIESTA Center, International Graduate School at Shenzhen, Tsinghua University, Shenzhen, P.R. China
[3] Biomanufacturing Engineering Laboratory, International Graduate School at Shenzhen, Tsinghua University, Shenzhen, P.R. China
[4] Institute of Optical Imaging and Sensing, Shenzhen Key Laboratory for Minimal Invasive Medical Technologies, Graduate School at Shenzhen, Tsinghua University, Shenzhen, P.R. China
[5] Key Laboratory of Wound Repair and Regeneration of PLA, Chinese PLA General Hospital, Medical College of PLA, Beijing, P.R. China
[6] Department of Mechanical Engineering, Biomanufacturing Center, Tsinghua University, Beijing, P.R. China
[7] Department of Mechanical Engineering, Drexel University, Philadelphia, PA, USA
[8] Biosciences Institute, Newcastle University

Correspondence: Siming Yang, Key Laboratory of Wound Repair and Regeneration of PLA, Chinese PLA General Hospital, Medical College of PLA, Beijing, P.R. China. e-mail: simingyang96@163.com
Wei Sun, Macromolecular Platforms for Translational Medicine and Bio-Manufacturing Laboratory, Tsinghua-Berkeley Shenzhen Institute, Shenzhen, P.R. China. e-mail: sun.wei@tsinghua.edu.cn
Shengli Mi, Open FIESTA Center, International Graduate School at Shenzhen, Tsinghua University, Shenzhen, P.R. China. e-mail: mi.shengli@sz.tsinghua.edu.cn

Received: May 21, 2020
Accepted: May 31, 2021
Published: December 22, 2021

Keywords: GelMA hydrogel; lamellar keratoplasty; Epithelial-to-mesenchymal transition; corneal stroma; regeneration

Citation: Chen Y, Dong L, Kong B, Huang Y, Zhong S, Connon C, Tan J, Yang S, Sun W, Mi S. Effects of gelatin methacrylate hydrogel on corneal repair and regeneration in rats. Transl Vis Sci Technol. 2021;10(14):25, https://doi.org/10.1167/tvst.10.14.25

Purpose: This study investigates the repairing process of rat cornea after surgery of lamellar keratoplasty (LKP) and evaluates the effects of gelatin methacrylate (GelMA) hydrogel.

Methods: In the LKP group, the lamellar stroma matrixes of Sprague-Dawley rats were transplanted to enhanced green fluorescent protein rats, whereas those in the GelMA group were also embedded with a GelMA hydrogel during the corneal transplantation. Grafted eyes were harvested on days seven, 30, and 90. Hematoxylin and eosin staining, immunofluorescence staining, scanning electron microscopy, optical coherence tomography, and a slit-lamp microscope were used to study the process of corneal restoration and regeneration.

Results: A total of 42 rats were analyzed, including 18 rats in each of the experimental group and six rats in the control group. After three months, the infiltration degree of inflammatory cells differed between the LKP group and the GelMA group ($P < 0.001$). Moreover, in multiple comparisons in corneal thickness, significant difference was observed between the LKP group and the GelMA group. There was also divergence in the results between the LKP group and the control group ($P < 0.001$, $P < 0.001$). At the same time, the expression of α-smooth muscle actin (α-SMA) and transforming growth factor (TGF)-β1 varied distinctly between the LKP group and the GelMA group ($P < 0.05$, $P < 0.001$).

Conclusions: Significant differences were demonstrated between the LKP group and the GelMA group in inflammatory cell infiltration, corneal thickness, as well as the expression of α-SMA and TGF-β1. Those differences indicate the ability of GelMA hydrogel to support alleviation in corneal stroma fibrosis and show the influences of fibrosis in the dysfunction of corneal refractive power.

Translational Relevance: Our research provides new ideas for the future development of LKP and tissue-engineered corneas.

Introduction

Corneal disease is the second-most blinding eye but reversible ophthalmology disease just after cataracts.[1,2] According to statistical results, more than 10 million people worldwide are blinded because of corneal diseases, of which corneal perforation is an ophthalmic emergency caused by traumatic, infectious, or immune keratopathy. Specifically, ocular trauma is the most common cause of corneal perforation, accounting for 67% of cases.[3] Corneal perforation destroys the integrity of the eyeball and changes the biophysical properties of the cornea. Compared with transplantation of other organs , cornea transplantation has the unique advantage of immune privilege.[4] Therefore, for treating corneal damage in worst-case scenarios, corneal transplantation is the only reliable and effective recovery treatment in clinical practice.

In the past 20 years, lamellar keratoplasty (LKP) has been widely adopted by corneal surgeons around the world. Because the posterior elastic membrane and endodermis are retained during the surgery,[5] postoperative rejection is relatively mild.

At present, many patients lose their vision because of the lack of corneal transplant material while suffering from corneal stromal damage or perforation. In addition, although cornea transplantation has immune privilege, approximately half of the patients still require immunosuppressive therapy after corneal allografting.[6,7] Even if the patient undergoes LKP, 3% to 24% of patients still experience immunological rejection after operation.[6,8,9] Therefore the lack of cornea donor and postoperative immune rejection are urgent problems to be solved. For these reasons, an increasing number of scholars have shifted their attention to alternative treatments for corneal transplantation, including transplanted corneal stem cell therapy, cell-free collagen scaffolds, tissue-engineered artificial corneas, and corneal prostheses.[10-13]

There are scholars who synthesized biodegradable polymer materials,[14,15] but these polymers are generally hydrophobic, thus greatly limiting their ability to encapsulate cells in the physiology structure. Hydrogel is a kind of water-rich polymeric material with a three-dimensional structure,[16] which is biomimetic to the extracellular matrix (ECM).[17] Since the structure of hydrogel is relatively suitable for cellular growth, it has been widely used to study the interaction between ECM and cells, as well as other cellular physiology such as cell proliferation, migration, and differentiation.[18,19] However, hydrogels are not an excellent choice for tissue-engineering materials due to the limitations of their mechanical strength. Therefore gelatin, which is a denatured product of collagen, is usually used to suit the needs in terms of physical properties. Gelatin methacrylate (GelMA) is a gelatin derivative[20] of the original gelatin, which is hydrophilic in properties. Compared to other biomaterials derived from hydrogels, GelMA can meet the biocompatibility and mechanical strength requirements for manufacturing biomaterials. GelMA is chemically tunable, biocompatible,[21] and biodegradable,[22] thereby providing a suitable living environment for a variety of cells. According to previous research, if cells are cultivated in a three-dimensional–structured hydrogel, they are able to reshape the environment around them for dissemination and migration.[23] These properties of GelMA meet the requirements for an ideal substrate for tissue-engineering scaffolds.[24]

Materials and Methods

Rat and Anesthesia

Sprague-Dawley (SD) rats were purchased from Guangdong Medical Laboratory Animal Center, China (Guangdong, China). Enhanced green fluorescent protein (EGFP) transgenic rats (SD background) were bought from Beijing Vital River Laboratory Animal Technology Co., Ltd (Beijing, China). To avoid the influence of gender in the experiment, all rats were female, eight to 12 weeks old, weighing 0.2 to 0.3 kg, and divided into two groups of nine each. Intrastromal keratoplasty was performed/implemented among them. All of the rats were treated according to standard protocols, and in compliance with the guidelines of the Animal Ethics Committee in Tsinghua University and the National Institutes of Health for the care and use of laboratory animals (NIH Publications no. 8023, revised 1978). Each rat was anesthetized by an intraperitoneal injection of 20 mg/kg pentobarbital sodium (Jiangxi Kelun Pharmaceutical Co., Ltd., Jiangxi, China) before all surgical procedures. The cornea of the EGFP rat is presented in green under excitation light, with the excitation optimal for EGFP close to 488 nm. Thus the cells originated from EGFP transgenic rats are suitable for analysis using the method of fluorescence microscopy.

Preparation of GelMA Hydrogel

Type-A gelatin powder 10 g (Sigma-Aldrich Corp., St. Louis, MO, USA) extracted from porcine skin was dissolved in 100 mL Dulbecco's phosphate-buffered saline (DPBS; Gibco, Thermo Fisher Scientific, Waltham, MA, USA) at 60°C. After having been

stirred at a rate of 0.1 mL/min for three hours, 6 mL methacrylic anhydride (MA; Sigma-Aldrich Corp.) was added to carry on the reaction at 50°C for four hours. The resulting mixture was then diluted to 1/5 with DPBS to stop the reaction. The resulting mixture was put through dialysis against the deionized water at 40°C for seven days, in the participating of a 12- to 14-kDa cutoff dialysis membrane. The pH of the mixture solution was adjusted to 7.4 by 1 M $NaHCO_3$ sterilized by a 0.2 µm syringe filter and freeze-dried for 72 hours, to obtain the GelMA sponge. GelMA sponge was dissolved in DPBS with 0.05% lithium phenyl-2,4,6-trimethyl-benzoyl phosphinate at 60°C, and exposed to 365 nm light for 90 seconds to obtain 5% (w/v) GelMA hydrogel. Luyor-365l (Luyor Instrument Co., Ltd, Irvine, CA, USA) was used in the experiment, with the light source of 10 mW/cm^2 radiation intensity. Samples were placed 5 cm away from the light source.

Hydrogel Degradation in Collagenase

GelMA hydrogels were equilibrated for one hour in 5 mL of 0.1 M Tris–HCl buffer (pH 7.4) that contained 5 mM $CaCl_2$ at 37°C. Subsequently, 125 CDU/mg of collagen was added to get a final collagenase solution of 5 U mL^{-1} concentration. The solution was replaced every eight hours. Moisture on the surface of the hydrogel was wiped dry before each weighing. The residual mass percentage of hydrogels was calculated according to the following equation:

$$\text{Residual Mass}\,\% = W_t/W_0,$$

where W_0 is the initial weight of the hydrogel and W_t is the weight of the hydrogel at every period of time.[25,26]

Surgical Methods and Graft Evaluation

In the LKP group, the anterior stroma was dissected by trephination, approximately 150 µm in depth and 3.0 mm in diameter, and we named the remaining rat cornea as recipient bed. Next, we implanted the allograft, approximately 150 µm in thickness and 3.5 mm in diameter, stitched to the recipient bed with eight interrupted sutures (10-0 nylon).

In the GelMA group, the anterior stroma was dissected by trephination, approximately 150 µm in depth and 3.0 mm in diameter. We then inserted a GelMA hydrogel, which is 100 µm in thickness and 2.0 mm in diameter, into the recipient bed. Next, we implanted the allograft, approximately 150 µm in thickness and 3.5 mm in diameter, and stitched it to the recipient bed with eight interrupted sutures (10-0 nylon).

In the last steps of the procedure, the eyelid was sutured to protect the transplanted corneas. Tobramycin-dexamethasone eyedrop (Alcon, Puurs, Belgium) was administered three times per day, and erythromycin eye ointment provided by Beijing Twinluck Pharmaceutical Co., Ltd. (Beijing, China) was administered once a day.

During the experiment, the operated cornea was photographed with a slit lamp (YZ5S; 66 Vision Tech, Jiangsu China) weekly, monthly, and quarterly after transplantation. Those showing immune rejection(vascularization) and lethal responses to anesthetic were excluded from the experiment.

Hematoxylin and Eosin Staining and Immunofluorescence

Corneal buttons from the LKP rats and GelMA hydrogel rats were fixed in 4% paraformaldehyde for eight hours, immersed in phosphate buffered saline solution for eight hours and immersed in 30% sucrose solution for eight hours. The dehydrated corneal buttons were embedded with OCT Compound (Tissue-Tek; SAKURA, Torrance, CA, USA) afterward. The frozen samples were cut into 8 µm–thick sections with a freezing microtome (CM1950; Leica, Wetzlar, Germany), and stained with an H&E Stain Kit (Baso, Zhuhai, China) according to the manufacturer's instructions. The resulting sections were then imaged with a light microscope (Leica). Before carrying out the immunofluorescence, tissue sections were incubated at 4°C overnight with anti–α-smooth muscle actin (anti–α-SMA) antibody (ab32575; Abcam, Cambridge, MA, USA) (1:500), transforming growth factor (TGF)-β1 (ab92486, Abcam) (1:500) and TGF-β3(ab15537; Abcam) (1:500). Negative controls were generated simultaneously by incubating sections without primary antibody. After a day, sections were incubated with anti-rabbit IgG(H+L) (Alexa Fluor 647–conjugate) (Cell Signaling Technology, Danvers, MA, USA) (1:1000) at 37°C for one hour in the dark, followed by three times of PBS rinsing for 10 minutes each, covered by anti-fade mounting medium (Solarbio) with 4′,6-diamidino-2-phenylindole (DAPI) (Cell Signaling Technology) and examined with a fluorescence microscope (Olympus, FV1000).

Optical Coherence Tomography (OCT) Observation

We applied the OCT equipment specially devised by the laboratory to visualize the cross-sections and thickness of the experimental rat cornea. The light

source is generated by superluminescent diode with a power of 15 mW and a center wavelength of 75 nm (Inphenix, Livermore, CA, USA). We chose a 2 × 2 fiber coupler with a split ratio of 50:50, to react as a Michelson interferometer, and finally, the spectrometer was assembled by a 1145 line/mm grating (Wasatch Photonics, Logan, UT, USA) and a GL2048R linear array CCD (Sensors Unlimited, Princeton, NJ, USA), respectively. The anesthetized rats were then mounted under the detector to obtain images.

Ultrastructure Analysis

The morphology of ECM and corneal collagen were imaged using the method of Scanning electron microscopy (SEM). Specimens were fixed in 2.5% glutaraldehyde for two hours, dehydrated by using an ethanol series at 4°C, washed five times with tertbutyl alcohol for 10 minutes each, and crystallized overnight in a freeze dryer (Freezone 4.5 L; Labconco Corporation, Kansas City, MO, USA). The samples were then imaged by SEM (Phenom XL; Phenom World, Shanghai, China).

Statistical Analyses

All of the experiments were performed at least three times. The statistical data are expressed as the means around ± 95% Confidence Interval. Student's *t*-test was applied to evaluate the effect of LKP and GelMA hydrogel for the regeneration of rat cornea. Subsequently, we used the function of IBM, SPSS, and Statistics 19 for analysis. $P < 0.05$ was considered significant, and $P < 0.01$ was considered statistically significant.

Results

In the LKP group, the lamellar stromal matrixes of SD rats were directly transplanted to EGFP rats, whereas the GelMA group was additionally embedded with a GelMA hydrogel during the corneal transplantation. By harvesting the grafts, we evaluated changes in the structure of corneal tissue after every operation, the degree of infiltration of the cells into the graft and the recipient bed, as well as tracked the changes in corneal cell morphology, regularly.

LKP and the Impact of GelMA

To observe the rat corneas after LKP and verify the effect of the GelMA hydrogel, the LKP group and the GelMA group underwent slit-lamp microscopy examinations on (a) day seven (weekly), (b) day 30 (monthly), and (c) day 90 (quarterly), respectively. During the quarterly (90-day) examination, neither of the transplantation groups showed postoperative complications such as immune rejection or vascularization, and all of the grafts remained completely clear.

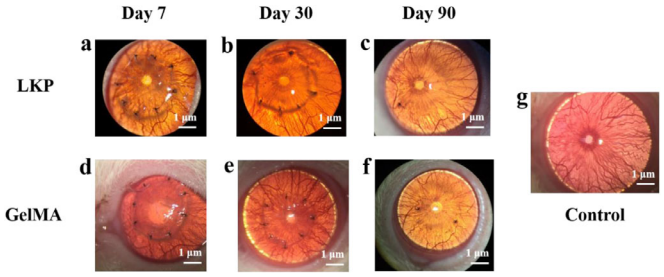

Figure 1. (a–f) Slit-Lamp Photography of LKP group and the GelMA group at days seven, 30, and 90 after operation. (g) Normal rat cornea. Magnification × 40. The experiments were repeated three times independently with similar results. The following figures showed the representative images.

Table 1. Thickness of Cornea After Operation

Group	Day 7 (n = 6)	Day 30 (n = 6)	Day 90 (n = 6)
LKP	721.21 ± 4.14	353.64 ± 9.05	181.60 ± 6.23
GeLMA	687.20 ± 10.05	286.58 ± 10.33	242.31 ± 5.33
Control	—	—	249.66 ± 4.44

Date are expressed as the mean ± 95% confidence interval.

One week after the operation, as shown in Figures 1a and 1d, corneal edema appeared in both the LKP rats and GelMA hydrogel rats. The cornea was slightly turbid, whereas the dividing line of the junction and the recipient bed was unobvious. One month after the operation, as shown in Figures 1b and 1e, the corneal edema was relieved, and the cornea tissue cleared up gradually. In addition, the GelMA hydrogels were relatively stable in properties, not likely to biodegrade rapidly in the collagenase biodegradation process (Supplementary Fig. S1). Three months after the operation, as shown in Figures 1c and 1f, the corneas of the LKP rats and the GelMA hydrogel rats recovered from turbidity, without any postoperative complications, such as immune responses or vascularization, and the GelMA hydrogel had largely degraded.

The corneal thickness on days seven, 30, and 90 after the operation are shown in Table 1 (The data were calculated as mean ± 95% Confidence Interval [n = 6]) and Figures 2a to 2f). We performed one-way analysis of variance of the corneal thickness measured by OCT in the experimental group, as shown in Supplementary Figures S2a and S2b), noticing that there was a significant difference between the LKP group and the GelMA group ($P < 0.001$). After three months of LKP, the corneal thickness of the LKP group, compared

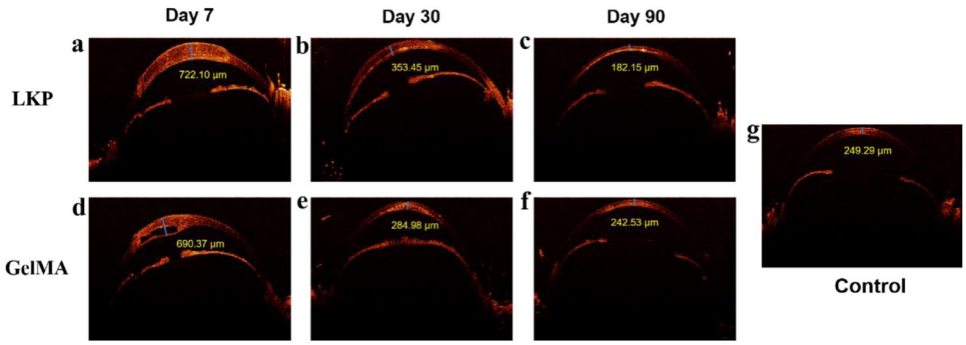

Figure 2. (a–f) OCT visualized the cornea thickness at days 7, 30, and 90 after operation. Normal rat corneas were used as the control group. (g) Normal rat cornea.

to the control group, was significantly reduced ($P < 0.001$). Bonferroni method was used to avoid false positives caused by multiple comparisons, with the result improving significantly after the correction. In addition, Student's *t*-testing was performed for the analysis between the corneal thickness of SD rats and EGFP rats ($P < 0.05$).

Characteristics of Corneal Tissue Structure

The inflammatory cell infiltration ratio of the recipient bed on days seven, 30, and 90 was calculated using Image J. The statistical results are shown in Table 2.

The inflammatory cell infiltration ratio refers to the proportion of the number of inflammatory cells clustered in the recipient bed to the total number of cells in the field of vision.

As shown in Figure 3, the infiltration ratio of inflammatory cells in the GelMA group rose initially, followed by a reduction, whereas that of the GelMA group gradually increased throughout.

We speculated that good adsorption of GelMA on the cells caused the corneal stromal cells around the damaged site to enter the GelMA hydrogel, leading to a greater number of inflammatory cells in the GelMA group than in the LKP group. Besides, early hydrogel swelling may also lead to unstable cell numbers.

Student's *t*-testing was performed on the inflammatory cell infiltration ratio, as shown in Figure 3i. We found that there was a significant difference between the LKP group and the GelMA group ($P < 0.001$). At three months after operation, the inflammatory cell infiltration ratio in the GelMA group, compared to the LKP group, was significantly reduced.

Table 2. Inflammatory Cell Infiltration Ratio (%)

Group	Day 7 (n = 6)	Day 30 (n = 6)	Day 90 (n = 6)
LKP	11.50 ± 0.96	12.81 ± 1.81	34.56 ± 5.23
GeLMA	14.69 ± 5.10	23.14 ± 5.96	16.75 ± 3.93
Control	0	0	0

Date are expressed as the mean ± 95% confidence interval.

We visually scored the SEM of the corneal microstructure on days seven, 30, and 90. The statistical results are shown in Table 3. The specific scoring rules and results are placed in the supplementary materials (Supplementary Table S1). As shown in Figures 4a to 4c, the number of corneal epithelial cells increased, the structure of the corneal stroma layer gradually returned to regularity, but almost zero new collagen fibers were visible. As shown in Figures 4d to 4f, the number of corneal epithelial cells increased, the structure of the corneal stromal layer gradually returned to normality, and there was obvious regeneration of collagen fibers.

Student's *t*-testing was performed on the scored SEM of the corneal microstructure, as shown in Figure 4h. However, we could not find a significant difference between the LKP group and the GelMA group.

Assessment of the Fate of Corneal Cells by Confocal Microscopy

Because the cells were relatively compact and the antibody signal was relatively dense, we chose the region expressing positive signal rather than the number of positive cells to quantify the antibody expression level. The positive cell area ratio represents the ratio of the antibody signaling region to the DAPI signaling region.

The α-SMA-positive area ratio of the LKP group was 48.02% ± 3.17%, whereas the α-SMA-positive area ratio of the GelMA group was 54.62% ± 5.31%. As shown in Figure 5, we used Student's *t*-test and found that the α-SMA positive area ratio of the LKP

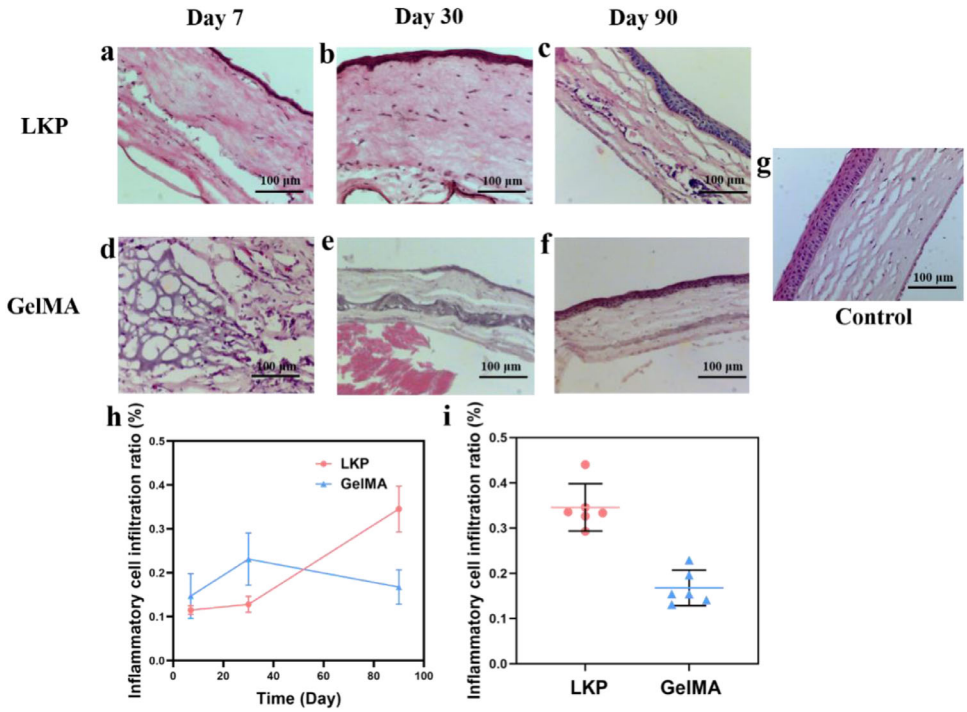

Figure 3. (a–f) Hematoxylin and eosin staining for the LKP rats and GelMA hydrogel rats on days seven, 30, and 90 after the operation. (g) Normal rat cornea. (h) Changes in inflammatory cell infiltration ratio of the LKP group and the GelMA group on days seven, 30, and 90 after operation. (i) Student's *t*-test was used to analyze the difference between the LKP group and the GelMA group. Magnification × 20. *Scale bar*: 100 μm. These are representative images (n = 6, biologically independent samples, biological replicates). Data are expressed as the mean ± 95% confidence interval. *$P < 0.05$; **$P < 0.01$; ***$P < 0.001$.

Table 3. SEM Visual Score of Corneal Microstructure

Group	Day 7 (n = 6)	Day 30 (n = 6)	Day 90 (n = 6)
LKP	0	2.83 ± 0.79	5
GeLMA	0	3.33 ± 0.54	6 ± 0.94
Control	9	9	9

Date are expressed as the mean ± 95% confidence interval.

group, compared to the GelMA group, was significantly reduced ($P < 0.05$), even though the α-SMA expression at the recipient bed was observed in the LKP group but not in the GelMA group.

Similar results also occurred in the expression of TGF-β1. The TGF-β1–positive area ratio of the LKP group was 9.83% ± 0.67%, whereas the TGF-β1–positive area ratio of the GelMA group was 30.01% ± 3.08%. According to Student's *t*-test, we discovered that the TGF-β1–positive area ratio of the LKP group, compared to the GelMA group, was significantly reduced ($P < 0.001$) (Supplementary Fig. S3).

Because of corneal development and regeneration, the expression of EGFP fluctuated differently. We performed the Student *t*-test on the expression of EGFP on days seven, 30, and 90, as shown in Figure 6, and found that there was a significant difference among the three periods. The Bonferroni method was used to avoid false-positive results caused by multiple comparisons, with the result improving after the correction. The expression of EGFP on day 30, compared to the expression of EGFP on day seven, increased significantly ($P < 0.001$). No significant difference was found between day 30 and day 90.

Discussion

This study established two models: the LKP group and the GelMA group. The GelMA group was additionally embedded with a GelMA hydrogel during corneal transplantation to explore the effects of the GelMA hydrogel on cell apoptosis and migration during the process of corneal repair. At the same time, the effects of the GelMA hydrogel on collagen fiber remodeling and cell signal factor expression during the repairing process were also reported and discussed.

The cornea is a transparent, nonvascular tissue located on the ocular surface, which is an important refractive component that affects vision,[27] and

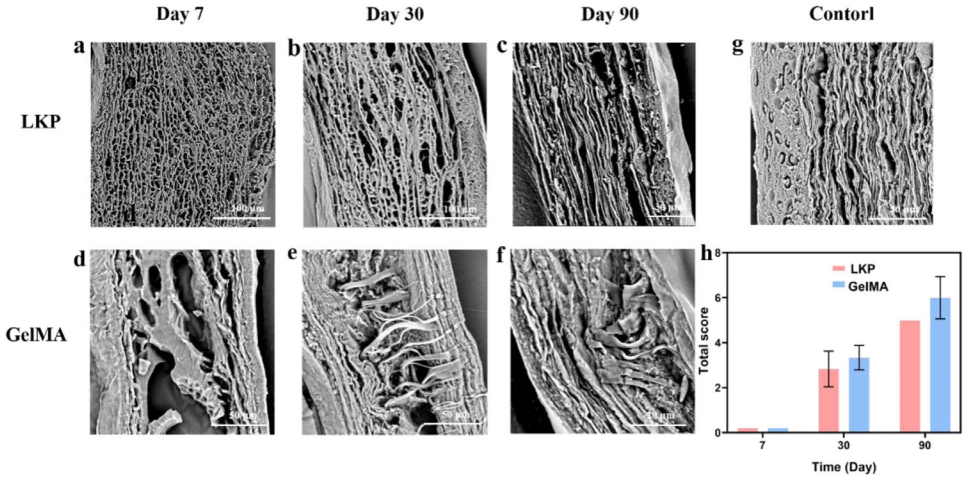

Figure 4. (a–f) SEM images of the LKP group and the GelMA group on days seven, 30, and 90 after operation. (g) Normal rat cornea as a control group. (h) Student's *t*-test was used to analyze the difference between the LKP group and the GelMA group on days 7, 30, and 90 after operation. These are representative images (n = 6, biologically independent samples, biological replicates). Data are expressed as the mean ± 95% confidence interval. *$P < 0.05$; **$P < 0.01$; ***$P < 0.001$.

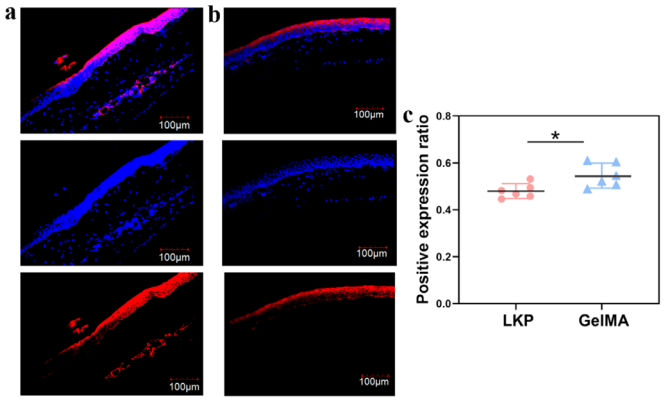

Figure 5. The *red marker* indicates α-SMA, and the *blue marker* indicates nuclei. (a) Immunofluorescence results for the LKP group on day 90. (b) Immunofluorescence results for the GelMA group on day 90. (c) Student's *t*-test was used to analyze the difference between the LKP group and the GelMA group for α-SMA expression. Magnification × 20. *Scale bar*: 100 μm. These are representative images (n = 6, biologically independent samples, biological replicates). Data are expressed as the mean ± 95% confidence interval. *$P < 0.05$; **$P < 0.01$; ***$P < 0.001$.

corneal epithelium is the outermost layer in the corneal structure. Because of the tight junctions (TJs) formed between corneal epithelial cells, harmful substances can be prevented from entering the corneal stroma.[28] However, the loss of the actin cytoskeleton can affect TJ formation, resulting in a lack of barrier function.[29]

The corneal epithelium is susceptible to physical, chemical, and biological factors that cause it to lose its barrier function. Therefore repair and regeneration of the cornea is essential for maintaining vision. In between, corneal injury can be repaired by various corneal refractive and transplant surgeries. However, the repairing procedures after corneal injury are complicated, including apoptosis, proliferation, migration, differentiation, and reconstruction of the ECM, which are affected and regulated by a number of factors.[30]

The regeneration process is divided into three phases: preparation for corneal damage repair, surface cell migration, and coverage over areas of epithelial defect, cell proliferation, and differentiation.[31] This complex regulatory process is usually regulated with precision by several antagonizing cytokine networks. Specifically, TGF-β1 subtypes regulate a variety of biological processes, including ECM synthesis, cell proliferation, apoptosis, and differentiation.[32] During the process of wound healing, TGF-β1 signaling is activated in corneal epithelial cells, which mediate Slug expression and Epithelial Mesenchymal Transition (EMT). Furthermore, TGF-β1 continuously upregulates Snail and Slug to maintain the EMT process in corneal epithelial cells and participates in corneal wound healing.[33] Subsequently, corneal epithelial cells migrate to the areas of epithelial defects through EMT, complete the re-coverage of the corneal epithelium, and improve the barrier function of the corneal epithelium. Therefore strengthening and speeding up the reconstruction of the corneal epithelial barrier could effectively reduce the occurrence of risks after surgery.

To ensure the transparency of the cornea, corneal epithelium prevents water from entering the corneal stroma from the outer environment, whereas the corneal endothelium prevents water from entering the stroma from the anterior chamber and pumps excess

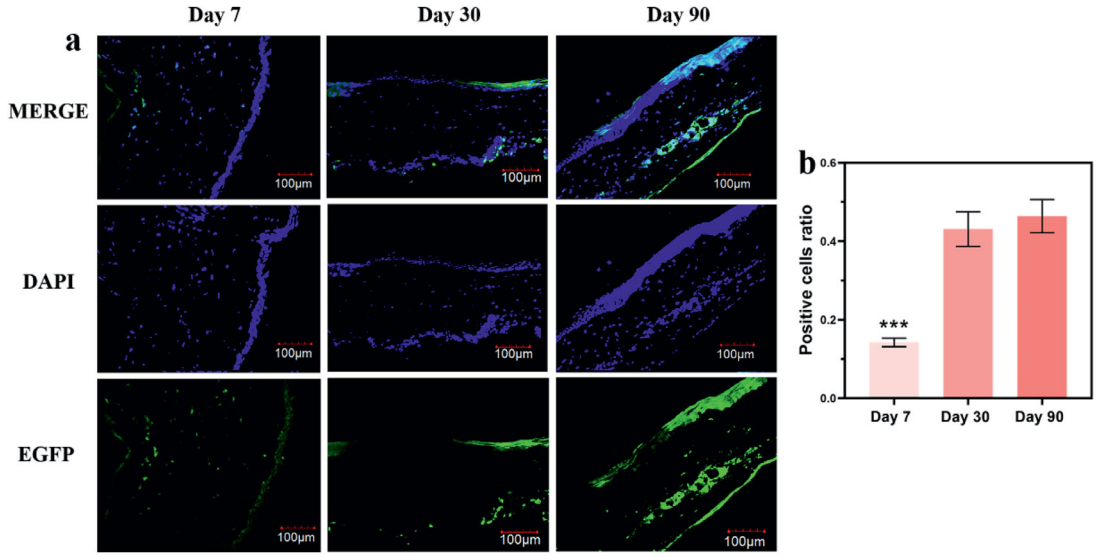

Figure 6. The *green marker* indicates EGFP, and the *blue marker* indicates nuclei. (a) Immunofluorescence results for the LKP group on day 90. (b) Immunofluorescence results for the GelMA group on day 90. (c) Bonferroni was used to analyze the difference between the LKP group and the GelMA group for α-SMA expression. Magnification $\times$ 20. *Scale bar*: 100 μm. These are representative images (n = 6, biologically independent samples, biological replicates). Data are expressed as the mean $\pm$ 95% confidence interval. *$P < 0.05$; **$P < 0.01$; ***$P < 0.001$.

water from the stroma into the anterior chamber.[34] In the first week after LKP, the corneal epithelium was damaged by surgery; thus the waterproofing function of the cornea was compromised and corneal edema occurred. The occurrence of edema destroys the regular and ordered lamellar structure of the corneal stroma, affecting the transparency of the cornea. Joshi et al.[35] developed a model that can be evaluated by in vivo imaging modalities, designing a model that combines the creation of stromal defect and the induction of controlled inflammatory insulted in the stromal bed by use of a rotating burr.

According to the experimental results, we witnessed that the corneal regeneration is divided into three phases: the apoptosis defense phase, the cell migration preparation phase, and the fibrotic repair phase. In the first week after LKP, the corneal lamellar graft was in contact with the recipient bed, and the corneal tissue went through the first stage of repair. Apoptosis occurred around the damaged site, forming an isolation zone to prevent other cells from infiltrating into the cornea. One month after LKP, corneal repair entered the second stage, where corneal stromal cells migrated to the damaged site, secreted ECM, and repaired the gap between the corneal lamellar graft and the recipient bed. At this stage, the corneal epithelium recovered, and the corneal waterproofing and barrier functions were restored. The cornea regained its clarity and transparency, and the laminar arrangement was basically restored to the corneal stroma. Three months after LKP, corneal regeneration entered the third stage. The keratocytes gathered at the junction of the corneal lamellar graft and the recipient bed differentiate into myofibroblasts, which functioned to remodel the stroma at the injury site. They secreted proteases to degrade the damaged stroma and other substrates for fibrotic repair. As a result, the corneal thickness was significantly reduced, and the refractive power of the cornea significantly improved compared to that of the normal cornea. At the same time, a large number of α-SMA signals were expressed in the corneal epithelium, as well as the junction of the graft and the recipient bed. The corneal structure basically went back to normal, except for the large number of myofibroblasts that accumulated at the junction of the corneal lamellar graft and the recipient bed and the large expression of special α-SMA in the corneal epithelium.

Interestingly, the presence of α-SMA markers in the corneal epithelium indicates that the corneal epithelial cells differentiated into myofibroblasts, which expressed a large amount of actin. We speculate that the high expression of actin functions as an emergency defense mechanism initiated by corneal tissue during the repair phase. First, it can strengthen the TJs between corneal epithelial cells to enhance the defensive properties of the corneal epithelium, protecting the damaged corneal stroma layer from external threats. Second, the characteristics of the myofibroblasts enhance the mechanical properties of

the corneal epithelium, thereby compensating for the damaged mechanical properties of the corneal stroma.

In addition, cytokines secreted by the corneal tissue promote the regeneration and repair of the cornea. Besides, TGF-β1 induces the EMT process in corneal epithelium, allows corneal epithelial cells to migrate to the defect area, and recovers the corneal epithelium.

Undeniably, GelMA hydrogel is an excellent tissue engineering material that is biocompatible, biodegradable, noncytotoxic, and nonimmunogenic. Cells can migrate and adhere to the surface of the GelMA hydrogel, maintaining good viability.[24] While inserting the GelMA hydrogel into the junction of the corneal lamellar graft and the recipient bed, we discovered some interesting phenomena. GelMA hydrogel rats and LKP rats showed different characteristics in the first week. Except for the occurrence of edema because of epithelium defects, the repair progress of the GelMA hydrogel rats was delayed compared to that of the LKP rats. For the possible reasons, we speculate that the GelMA hydrogel functioned to prevent corneal lamellar graft and the recipient bed from directly contacting each other, so that the keratocytes failed to recognize the circumstances and caused the corneal repair phase to be postponed.

Notably, one month after surgery was performed, the corneal tissue appeared to approach the GelMA hydrogel. As shown in Figure 4, by growing fibers that crossed the corneal stroma layer, the graft was able to connect to the recipient bed. Meanwhile, the thickness of GelMA hydrogel decreased compared to that after the operation.

Unlike the one-month results of the LKP group, cell aggregation was not observed around the junction of the graft and the recipient bed in the GelMA hydrogel rats. Cells that entered the GelMA hydrogel may have inhibited the differentiation of the keratocytes into myofibroblasts at the junction of the graft and the recipient bed, thus impeding fibrotic repair of the cornea. Three months after the operation, myofibroblasts at the junction of the graft and the recipient bed remained invisible, whereas the fibrotic repair of the cornea was suppressed. Based on the results of OCT, the corneal thickness and refractive power were similar to those of the normal cornea. However, the specific mechanism of the phenomenon needs to be clarified with further experiments.

The application of GelMA hydrogels might be a long way off from clinical practice, but they have the potential to be one of the most promising candidates for tissue repairing components.[36] However, there is still a need to develop hydrogels with increased compatibility between the hydrogels and the tissue defects in clinical practice. Second, GelMA hydrogels are not strong enough in terms of mechanical properties; hence, they are unable to fully meet the modulus values of the native cornea.[37] Therefore the mechanical strength of GelMA hydrogels should be improved by altering the cross-linking times, energies, and other parameters.

Besides, although conventional allograft therapy for corneal scarring is widespread and successful, the donor tissue is not readily available. Several grafts failed because of rejection and complications such as endothelial failure. Under such circumstances, treating with autologous stem cells will be a more appropriate therapy. Specifically, mesenchymal cells should be expanded from small superficial, clinically replicable limbal biopsy specimens of human cadaveric corneoscleral rims. Recently, the presence of biopsy-derived stromal cells induced regeneration of ablated stroma, with tissue exhibiting lamellar structure and collagen organization, which is indistinguishable from that of native tissue. Limbal biopsy-derived stromal cells, which are capable of corneal stromal remodeling, can be expanded under xeno-free autologous conditions. They present a potential for autologous stem cell-based treatment of corneal stromal blindness.[38]

In summary, the insertion of the GelMA hydrogel improves the performance of corneal repair process, and functions to inhibit corneal fibrosis repair during the post-surgery repair of corneal transplantation. The effect might be related to the regulation of the TGF-β1 pathway. Therefore GelMA hydrogel not only is a suitable application in the field of tissue engineering, it also has the potential as a new auxiliary material in corneal transplantation surgery.

Conclusions

In conclusion, we discovered that the graft in the host is still surviving but was symbiotic with the host cornea. The insertion of a GelMA hydrogel helps to alleviate the phenomenon of corneal stroma fibrosis and reduces the loss of corneal refractive power caused by fibrosis. Our research not only provides new ideas for the future development for the biomaterial selection in lamellar keratoplasty but also suggest a potential application of tissue-engineered corneas.

Acknowledgments

Supported by the National Key Research and Development Program of China (No.2018YFC1106000), the Key Research and Devel-

opment Projects of People's Liberation Army (No. BWS17J036), and the Project of Basic Research of Shenzhen, China (JCYJ20170412101508433 &JCYJ20180507183655307).

Disclosure: **Y. Chen,** None; **L. Dong,** None; **B. Kong,** None; **Y. Huang,** None; **S. Zhong,** None; **C. Connon,** None; **J. Tan,** None; **S. Yang,** None; **W. Sun,** None; **S. Mi,** None

[#] YC and LD contributed equally to this work.

References

1. Negrel AD, Thylefors B. The global impact of eye injuries. *Ophthal Epidemiol*. 1998;5:143–169.
2. Jhanji V, Young AL, Mehta JS, Sharma N, Agarwal T, Vajpayee RB. Management of corneal perforation. *Surv Ophthalmol.* 2011;56:522–538.
3. Xie L, Zhai H, Dong X, Shi W. Primary diseases of corneal perforation in Shandong Province, China: a 10-year retrospective study. *Am J Ophthalmol*. 2008;145:662–666.
4. Armitage WJ, Jones MN, Zambrano I, Carley F, Tole DM, Group NOTA, Contributing Ophthalmologists OAS. The suitability of corneas stored by organ culture for penetrating keratoplasty and influence of donor and recipient factors on 5-year graft survival. *Invest Ophthalmol Vis Sci*. 2014;55:784–791.
5. Guilbert E, Bullet J, Sandali O, Basli E, Laroche L, Borderie VM. Long-term rejection incidence and reversibility after penetrating and lamellar keratoplasty. *Am J Ophthalmol*. 2013;155:560–569.
6. Cursiefen C. Immune privilege and angiogenic privilege of the cornea. *Chem Immunol Allergy*. 2007;92:50–57.
7. Kumar P, Pandit A, Zeugolis DI. Progress in corneal stromal repair: from tissue grafts and biomaterials to modular supramolecular tissue-like assemblies. *Adv Mater*. 2016;28:5381–5399.
8. Liu H, Chen Y, Wang P, Sheng M, et al. Efficacy and safety of deep anterior lamellar keratoplasty vs. penetrating keratoplasty for keratoconus: a meta-analysis. *Plos One*. 2015;10:1–14.
9. Yam HF, Yusoff NZBM, Goh TW, et al. Decellularization of human stromal refractive lenticules for corneal tissue engineering. *Sci Rep*. 2016;6:26339–26350.
10. Pinnamaneni N, Funderburgh JL. Concise review: Stem cells in the corneal stroma. *Stem Cells*. 2012;30:1059–1063.
11. Donald T, et al. Ophthalmology 3 Corneal transplantation. *Lancet.* 2012;379(9827):1749–1761.
12. Polisetti N, Islam MM, Griffith M. The artificial cornea. *Methods Mol Biol.* 2013,1014:45–52.
13. Wu J, Du Y, Mann MM, et al. Bioengineering organized, multilamellar human corneal stromal tissue by growth factor supplementation on highly aligned synthetic substrates. *Tissue Eng Part A*. 2013;19(17-18):2063–2075.
14. Bettinger CJ, Bruggeman JP, Borenstein JT, Langer RS. Amino alcohol-based degradable poly (ester amide) elastomers. *Biomaterials*. 2008;29:2315–2325.
15. Bruggeman JP, Bruin B, Bettinger CJ, Langer R. Biodegradable poly (polyol sebacate) polymers. *Biomaterials.* 2008;29:4726–4735.
16. Dubruel P, Schacht E, Van Vlierberghe S. Biopolymer-based hydrogels as scaffolds for tissue engineering applications: a review. *Biomacromolecules*. 2001;12:1387–1408.
17. Serafim A, Tucureanu C, Petre D-G, et al. One-pot synthesis of superabsorbent hybrid hydrogels based on methacrylamide gelatin and polyacrylamide. Effortless control of hydrogel properties through composition design. *New J Chem.* 2014;38(7):3112–3126.
18. Luo Y, Shoichet MS. A photolabile hydrogel for guided three-dimensional cell growth and migration. *Nat Mater*. 2004;3:249–253.
19. West LJ. Protein-patterned hydrogels: customized cell microenvironments. *Nat Mater.* 2011;10(10):727–729.
20. Bulcke AI, Bogdanov B, De Rooze N, et al. Structural and rheological properties of methacrylamide modified gelatin hydrogels. *Biomacromolecule.* 2000;1:31–38.
21. Powell MF. Stability of lidocaine in aqueous solution: effect of temperature, pH, buffer, and metal ions on amide hydrolysis. *Pharm Res-Dordr.* 1987;4:42–45.
22. Ratcliffe JH, Hunneyball IM, Smith A, et al. Preparation and evaluation of biodegradable polymeric systems for the intra-articular delivery of drugs. *J Pharm Pharmacol*. 1984;36:431–436.
23. Benton JA, DeForest CA, Vivekanandan V, et al. Photocrosslinking of gelatin macromers to synthesize porous hydrogels that promote valvular interstitial cell function. *Tissue Eng Part A.* 2009;15:3221–3230.
24. Knopf-Marques H, Barthes J, Wolfova L, et al. Auxiliary biomembranes as a directional delivery system to control biological events in cell-laden tissue-engineering scaffolds. *ACS Omega.* 2017;2:918–929.

25. Mirazul M, Ravichandran R, Olsen D, et al. Self-assembled collagen-like-peptide implants as alternatives to human donor corneal transplantation. *Rsc Adv*. 2016;6:55745–55749.
26. Jangamreddy JR, Haagdorens MKC, Mirazul Islam M, et al. Short peptide analogs as alternatives to collagen in pro-regenerative corneal implants. *Acta Biomater.* 2018;69:120–130.
27. Meek KM, Knupp C. Corneal structure and transparency. *Prog Retin Eye Res*. 2015;49:1–16.
28. Prada J, Noelle B, Baatz H, Hartmann C, Pleyer U. Tumour necrosis factor alpha and interleukin 6 gene expression in keratocytes from patients with rheumatoid corneal ulcerations. *Br J Ophthalmol.* 2003;87:548–550.
29. Turner JR. "Putting the squeeze" on the tight junction: understanding cytoskeletal regulation. *Semin Cell Dev Biol*. 2000;11:301–308.
30. Ljubimov AV, Saghizadeh M. Progress in corneal wound healing. *Prog Retin Eye Res*. 2015;49:17–45.
31. Ma A, Zhao B, Boulton M, Albon J. A role for Notch signaling in corneal wound healing. *Wound Repair Regen*. 2011;19(1):98–106.
32. Roberts AB. The ever-increasing complexity of TGF-beta signaling. *Cytokine Growth Factor Rev.* 2002;13:3–5.
33. Aomatsu K, Arao T, Abe K, et al. Slug is upregulated during wound healing and regulates cellular phenotypes in corneal epithelial cells. *Invest Ophthalmol Vis Sci*. 2012;53:751–756.
34. Miguel M P D, Alio J L, Arnalich-Montiel F, et al. Cornea and ocular surface treatment. *Curr Stem Cell Res T*. 2010;5:195–204.
35. Joshi VP, Vaishnavi K S, Ojha SK, et al. A reliable animal model of corneal stromal opacity: Development and validation using in vivo imaging. *Ocul Surf*. 2020;18:681–688.
36. Uyaniklar M, Günal Gülin, Tevlek A , *et al.* A hybrid cornea: cell laden hydrogel incorporated decellularized matrix. *ACS Biomater Sci Eng.* 2020;6:122−133.
37. Sun M, Sun X, Wang Z, et al. Synthesis and properties of gelatin methacryloyl (gelma) hydrogels and their recent applications in load-bearing tissue, *Polymers.* 2018;10:1290–1310.
38. Basu S, Hertsenberg A J, Funderburgh M L, et al. Human limbal biopsy–derived stromal stem cells prevent corneal scarring. *Sci Transl Med.* 2014;6(266):172–182.